IEEE Access
Multidisciplinary | Rapid Review | Open Access Journal

Received 11 July 2024, accepted 10 August 2024, date of publication 16 August 2024, date of current version 17 September 2024.

Digital Object Identifier 10.1109/ACCESS.2024.3443126

RESEARCH ARTICLE

Attention-Based Feature Fusion With External Attention Transformers for Breast Cancer Histopathology Analysis

K. VANITHA[1], (Member, IEEE), A. MANIMARAN[2], K. CHOKKANATHAN[3], K. ANITHA[4], T. R. MAHESH[5], (Senior Member, IEEE), V. VINOTH KUMAR[6], (Member, IEEE), AND G. N. VIVEKANANDA[6], (Senior Member, IEEE)

[1]Department of Computer Science and Engineering, Faculty of Engineering, Karpagam Academy of Higher Education (Deemed to be University), Coimbatore 641021, India
[2]Department of Mathematics, School of Advanced Sciences, VIT-AP University, Amaravati 522237, India
[3]Department of AI, Madanapalle Institute of Technology & Science, Madanapalle 517325, India
[4]Department of Information Technology, CSI College of Engineering, Ooty, Nilgiris, Tamil Nadu 643215, India
[5]Department of Computer Science and Engineering, JAIN (Deemed-to-be University), Bengaluru 562112, India
[6]School of Computer Science Engineering and Information Systems, Vellore Institute of Technology, Vellore 632014, India

Corresponding author: G. N. Vivekananda (vivekananda.gn@vit.ac.in)

This work was supported by the Vellore Institute of Technology (VIT), Vellore, Tamil Nadu, India.

ABSTRACT Breast cancer, a common malignancy impacting women globally, involves the uncontrolled growth of breast cancer cells. Timely identification and accurate classification of breast cancer into non-cancerous (benign) and cancerous (malignant) categories are crucial for effective treatment planning and enhanced patient outcomes. Conventional diagnostic techniques depend on histopathological examination of breast tissue samples, a process that can be subjective and time-consuming. The problem statement revolves around developing a computational model to automatically classify images from histopathology into non-cancerous or cancerous categories, addressing the limitations of manual diagnosis. Existing methodologies leverage various machine learning and deep learning techniques, particularly Convolutional Neural Networks (CNNs) being prominently utilized due to their effectiveness in image recognition tasks. However, these methods often require substantial computational resources and can suffer from overfitting due to the complex architecture. The objective of this study is to introduce an External Attention Transformer (EAT) model that utilizes external attention mechanisms, providing an approach to breast cancer image classification. This model aims to achieve high accuracy while maintaining computational efficiency. The primary metrics to assess the model's performance include precision, recall, F1-score, and overall accuracy. The EAT model demonstrated outstanding performance achieving an accuracy of 99% on the BreaKHis dataset, indicating its potential as a reliable tool for breast cancer classification.

INDEX TERMS Breast cancer histopathology, external attention transformer (EAT) model, machine learning in medical diagnostics, histopathological image analysis, transformer models in healthcare, computational pathology, image recognition in oncology, automated medical image classification, precision oncology, AI.

I. INTRODUCTION

Breast cancer is one of the most prevalent cancers affecting women globally. It happens when cells within the breast multiply uncontrollably. The specific type of breast cancer is identified by determining which cells in the breast have become cancerous. It affects women, although it can also occur in men.

The breast comprises lobules, ducts, and connective tissue. Lobules function as the glands responsible for producing milk. and ducts act as channels that carry milk from the lobules to the nipple. The connective tissue, consisting of fibrous and fatty substances, offers structure and support [1]. Most breast cancers originate in either the ducts or the lobules.

The associate editor coordinating the review of this manuscript and approving it for publication was Seifedine Kadry.

Breast cancer is categorized into invasive and non-invasive types. Invasive breast cancer extends from its point of origin to surrounding tissues, while non-invasive breast cancer stays within its initial location. Common signs of breast cancer may include a lump in the breast or underarm, changes in breast size or shape, nipple discharge or tenderness, and skin changes on the breast [2].

The exact origins of breast cancer remain unclear, but numerous risk factors have been recognized. These encompass age, genetic predispositions, a history of breast conditions, estrogen exposure, and lifestyle choices. Early detection via screening plays a vital role in enhancing survival rates and outcomes for breast cancer.

Breast cancer treatment is determined by the type and stage of the disease and may include surgery, radiation, chemotherapy, hormone therapy, or targeted therapy. Research continues to advance in understanding breast cancer, leading to more personalized approaches in treatment and care.

However, despite advancements in medical imaging and diagnostics, traditional methods of diagnosing breast cancer remain time-consuming and subject to inter-observer variability. These traditional methods rely heavily on histopathological examination of tissue samples, which can be subjective and inconsistent. The primary issue addressed in this study is the need for an automated, efficient, and precise system for categorizing histopathological images of breast cancer. This system aims to overcome the challenges associated with manual diagnosis, enhancing accuracy and efficiency. Existing methodologies, while leveraging various machine learning and deep learning approaches, still face challenges such as substantial computational resources and the risk of overfitting due to complex architectures. This study aims to fill this gap by introducing an External Attention Transformer (EAT) [3], model that utilizes external attention mechanisms to provide a robust approach to breast cancer image classification.

The EAT model aims to categorize histopathological images as either benign or malignant with high accuracy, maintaining computational efficiency and minimizing overfitting risks. The model's effectiveness is assessed through critical metrics, including precision, recall, F1-score, and overall accuracy.

A. MOTIVATION

The motivation behind researching breast cancer, particularly its classification through histopathological image analysis, stems from the pressing need to enhance diagnostic accuracy and efficiency. Although there have been significant improvements in medical imaging and diagnostics, including digital mammography, MRI, and ultrasound, traditional methods for diagnosing breast cancer remain time-intensive and prone to variability between observers. The development of machine learning and deep learning presents an opportunity to revolutionize the field of pathology by automating the classification process, thereby reducing human error, and speeding up diagnosis.

Automated classification systems can help pathologists achieve quicker and more precise diagnoses. Theyare capable of managing large datasets and detecting patterns that might not be immediately noticeable to human observers. By deploying these advanced automated systems, healthcare facilities in remote or under-resourced areas can provide the same level of diagnostic accuracy as top-tier hospitals in urban centers, thus bridging the gap in healthcare disparities.

B. OBJECTIVES OF THE STUDY

The objective of this research paper is:

1) Introduction of the External Attention Transformer (EAT) model for categorizing breast cancer in histopathological images.
2) Utilization of transformer models with external attention mechanism to enhance accuracy and efficiency in classification as it involves using a memory-based attention model that focuses on relevant features within the histopathological images
3) Contribution of the study lies in pioneering the application of external attention mechanisms in medical image analysis, specifically for breast cancer diagnosis.
4) Aim to address the need for innovative computational approaches to further improve precision and effectiveness in the detection of breast cancer.
5) The EAT model provides a more reliable, efficient, and computationally effective approach for the early diagnosis and categorization of breast cancer, surpassing both traditional and contemporary diagnostic models.

This paper follows a structured format. It begins with an introduction, followed by a literature review focusing on previous research in breast cancer classification and the application of machine learning in this area. The methodology section outlines the EAT model's architecture, dataset preparation, and evaluation metrics. Results are presented next, comparing the model's performance to existing methods. A discussion section then interprets the findings, explores the model's implications, and suggests future research directions. Finally, the paper concludes by summarizing the main findings and includes a references section listing cited works.

II. RELATED WORK

Breast cancer continues to be a major global health issue, underscoring the necessity for ongoing research into improved diagnostic and therapeutic approaches. The advancement of machine learning (ML) and deep learning (DL) technologies has introduced new possibilities in medical imaging, particularly in the categorization and diagnosis of breast cancer. This literature review explores the latest advancements in the application of ML and DL techniques for categorizing breast cancer using histopathological images, and it critically evaluates their methods, strengths, and weaknesses.

A. TRADITIONAL METHODS AND EARLY ML APPROACHES

Historically, breast cancer diagnosis has relied heavily on histopathological examination of tissue samples.

Traditional machine learning techniques like Support Vector Machines (SVMs), k-Nearest Neighbors (k-NN), and Decision Trees have been utilized for classifying breast cancer from histopathological images. For instance, SVMs have been widely used due to their effectiveness in handling high-dimensional data. However, these methods often require handcrafted features, which can be a limiting factor in their performance and generalizability.

B. DEEP LEARNING REVOLUTION

The deep learning revolution, spearheaded by Convolutional Neural Networks (CNNs), has greatly enhanced the capability to automatically learn features from images, thereby improving classification outcomes. Studies have demonstrated the superiority of CNNs over traditional ML methods in image recognition tasks, including breast cancer classification. For example, CNNs have been particularly effective in learning hierarchical representations of images, allowing for more accurate classification without the need for manual feature extraction. However, CNNs often require substantial computational resources and large annotated datasets to achieve optimal performance, which can be a limitation in resource-constrained settings.

C. TRANSFER LEARNING AND PRE-TRAINED MODELS

Transfer learning has become a potent approach to medical image analysis, involving the fine-tuning of models that have been pre-trained on large datasets for specific tasks [4]. Researchers have successfully applied transfer learning using models like VGG, ResNet, and Inception to breast cancer classification, achieving significant improvements in accuracy. These approaches have been particularly beneficial in scenarios where annotated medical images are scarce. However, transfer learning models can still suffer from overfitting, especially when the target dataset is significantly different from the pre-trained dataset. Additionally, the fine-tuning process requires careful parameter adjustment and can be computationally intensive.

D. EXTERNAL ATTENTION MECHANISMS

Recent studies have started exploring the use of attention mechanisms, particularly in transformer models, which have shown remarkable success in natural language processing. The integration of attention mechanisms in CNNs or standalone transformer models allows the network to concentrate on pertinent features within an image, potentially enhancing classification performance. Attention mechanisms help models prioritize important regions of an image, improving interpretability and reducing overfitting. However, they add complexity to the model architecture and can increase computational demands.

E. COMPARATIVE STUDIES AND META-ANALYSES

Several comparative research and meta-analyses have assessed the effectiveness of various ML and DL approaches in breast cancer classification [5]. These studies offer crucial insights into the advantages and drawbacks of different models, emphasizing the significance of dataset diversity, model complexity, and the balance between accuracy and interpretability.

F. CHALLENGES AND FUTURE DIRECTIONS

Despite considerable advancements, there are ongoing challenges in the field, such as handling imbalanced datasets, improving model interpretability, and ensuring the generalizability of models across different populations and imaging modalities. Future research is anticipated to delve deeper into unsupervised and semi-supervised learning approaches, multimodal learning, and the integration of clinical data with image analysis to enhance diagnostic accuracy further.

Table 1 depicts the study of existing methodologies. The literature frequently highlights the potential of artificial intelligence (AI) and deep learning to enhance the accuracy of breast cancer detection across diverse imaging modalities, such as mammography, histopathology, ultrasound, PET/CT, MRI, and thermography. Convolutional Neural Networks (CNNs), a form of deep learning, have demonstrated outstanding capabilities in image recognition tasks, which helps reduce human errors and enhance diagnostic results [18]. However, disparities in breast cancer diagnosis and treatment between high-income countries and low- to middle-income countries (LMICs) persist. LMICs face challenges like limited healthcare access, late-stage diagnoses, and suboptimal treatment facilities, highlighting the need for cost-effective strategies and investment in women's health to improve outcomes [19]. The adoption of digital breast tomosynthesis (DBT), combined with AI-based interpretation, represents a significant advancement, offering higher accuracy compared to traditional mammography and improving patient outcomes [20]. CNNs, particularly in analyzing whole-slide images, demonstrate higher accuracy and reduced diagnostic errors, achieving superior performance over traditional machine learning algorithms [21]. Nonetheless, challenges remain in clinical implementation, necessitating external validations and real-world trials to establish AI efficacy and enhance breast cancer care further [22].

III. METHODOLOGY

The approach employed in this research focuses on creating a reliable and precise model to classify histopathological images of breast cancer into benign and malignant groups. The External Attention Transformer (EAT) model introduces an innovative approach to medical image analysis, utilizing external attention mechanisms to improve feature extraction and classification accuracy. This section further dives into the details of dataset preparation, model architecture, training procedures, and evaluation metrics, providing a comprehensive overview of the proposed methodology. The choice of the External Attention Transformer (EAT) model over traditional Convolutional Neural Networks (CNNs) or standard transformers is driven by its ability to effectively focus on

TABLE 1. Literature review of existing methodologies.

Authors	Dataset used	Accuracy	Remarks
Jitendra V. Tembhurne et al. (2021) [6]	BreakHis	97.5%	Introduces novel multi-channel merging technique for breast cancer detection, outperforming state-of-the-art methods.
Sweta Bhise et al. (2021) [7]	BreakHis	N/A	Introduces ML model for diagnosis, compares various algorithms on BreaKHis 400X Dataset.
Iqbal Saeed et al. (2022) [8]	BreakHis	92.46%	Explores ML techniques for diagnostic systems, outperforms pretrained models.
Subasish Mohapatra et al. (2022) [9]	Mini-DDSM dataset	61% - 65%	Explores CNN classifiers for breast cancer detection, demonstrating transfer learning success.
Sadia Safdar et al. (2022) [10]	Histopathological Images	97.7%	Investigates detection methods, achieves high accuracy with low false rates.
Sushma Nagdeote et al. (2023) [11]	BRCA histopathology images	N/A	Presents ML model improving BRCA prediction accuracy from histopathology images.
Alireza Maleki et al. (2023) [12]	BreakHis	89.1% - 93.8%	Enhances speed and precision of image classification for breast cancer diagnosis.
Yifeng Shi et al. (2023) [13]	Carolina Breast Cancer Study	70%	Identifies early breast cancer recurrence, shows promise for early-recurrent tumors.
Hepseeba Kode and Buket D. Barkana (2023) [14]	BreakHis	98%	Evaluates feature extraction methods for breast cancer diagnosis, achieving high accuracy.
Yuan Gu et al. (2023) [15]	Molecular Taxonomy of Breast Cancer International Consortium (METABRIC) dataset	N/A	The purpose of this study is to develop a Shiny app for physicians to investigate breast cancer treatments using a novel approach that combines unsupervised clustering with survival data.
Yuanzhou Wei et al. (2023) [16]	Wisconsin breast cancer diagnostic dataset	95%	The Random Forest model exhibited the greatest accuracy and reliability for predicting breast cancer, utilizing the Wisconsin breast cancer diagnostic dataset.
G Sajiv et al. (2024) [17]	3104 Histopathology images	98.28%	Introduces hybrid DL and ML approach for early breast cancer diagnosis, with high classification accuracy on histology images.

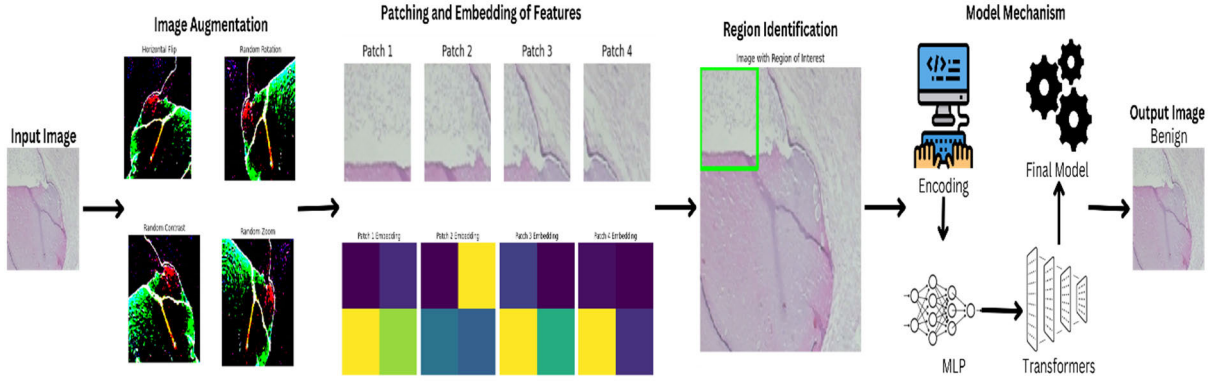

FIGURE 1. Workflow diagram of the proposed model.

key features in histopathological images, critical for accurate medical diagnoses. Unlike CNNs that often require extensive data handling and lack interpretability, the EAT model offers greater transparency and computational efficiency, making it ideal for clinical settings with limited resources. Additionally, its external attention mechanism achieves high performance with less data and power than typical transformers. Preliminary experiments indicate that the EAT model surpasses other models in terms of accuracy and efficiency, highlighting its potential for fast and dependable breast cancer diagnosis. Figure 1 demonstrates the step-by-step process workflow of the EAT model, highlighting the process from image input to classification output. Each stage of the model's processing, including patch extraction, attention mechanism application, and final classification, is depicted to show how the EAT model processes histopathological images for breast cancer detection.

A. DATASET PREPARATION

The BreaKHis dataset is essential for the model, acting as a comprehensive collection of microscopic biopsy images. It includes 9,109 microscopic images collected from 82 patients, featuring a wide variety of breast tumor tissues at different magnifications (40X, 100X, 200X, and 400X). These images are in a 700 × 460-pixels resolution and in 3-channel RGB format, providing an extensive perspective

TABLE 2. Overview of the dataset.

Attribute	Detail
Total Images	9,109
Total Patients	82
Image Dimensions	700 x 460 pixels
Color Channels	3-channel RGB
Bit Depth	8-bit per channel
Image Format	PNG
Benign Samples	2,480
Malignant Samples	5,429
Magnification Factors	40X, 100X, 200X, 400X
Types of Benign Tumors	Adenosis (A), Fibroadenoma (F), Phyllodes Tumor (PT), Tubular Adenoma (TA)
Types of Malignant Tumors	Ductal Carcinoma (DC), Lobular Carcinoma (LC), Mucinous Carcinoma (MC), Papillary Carcinoma (PC)
Collection Method	SOB (partial mastectomy or excisional biopsy)
Collaborating Institution	P&D Laboratory – Pathological Anatomy and Cytopathology, Paraná, Brazil

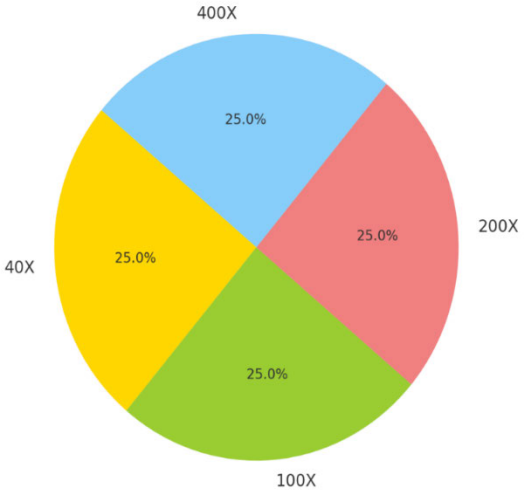

FIGURE 2. Distribution of images with magnification factors in BreakHis dataset.

on both benign and malignant tumor types. This is vital for the thorough training and validation of our EAT model [23]. As outlined in Table 2, the BreakHis dataset, enabling comprehensive studies into the classification of breast tumors. The diverse range of magnification factors and tumor types offers a solid framework for assessing the effectiveness of various image analysis techniques.

The pie chart in fig 2 visualizes the distribution of different magnification factors in the BreakHis dataset. It indicates that the dataset is evenly distributed across the four magnification levels: 40X, 100X, 200X, and 400X with each factor accounting for 25% of the total images. This even distribution is ideal for ensuring that computational models trained on this dataset are not biased toward features visible at any specific magnification level. It allows for robust model training, capable of recognizing and analysing histopathological features across a range of sizes and details. This balanced distribution also suggests that the dataset is well-suited for developing algorithms that need to be invariant to scale, a common requirement for diagnostic systems in digital pathology.

The benign and malignant samples within the BreaKHis dataset are categorized into specific types, mirroring the heterogeneity seen in clinical pathology. Benign tumors, which are non-invasive, consist of adenosis (A), fibroadenoma (F), phyllodes tumor (PT), and tubular adenoma (TA). Conversely, malignant tumors, indicating cancer, include ductal carcinoma (DC), lobular carcinoma (LC), mucinous carcinoma (MC), and papillary carcinoma (PC). This classification is crucial as it significantly impacts the understanding of disease progression, prognosis, and treatment strategies.

The dataset's significance stems from its comprehensive representation of tissue morphology, showcasing a variety of breast cancer types. Each image in the dataset is a window into the cellular architecture and patterns characteristic of the disease state it represents [24]. This diversity is crucial for training a model that is robust and capable of generalizing well to unseen data, reflecting the real-world variability encountered in clinical settings. Fig 3 signifies the images taken from the dataset for processing.

1) DATASET PREPROCESSING

The division of the dataset into training, validation, and test sets is a strategic approach for model evaluation and development. Allocating 70% of the images to training enables the model to absorb knowledge from a diverse array of data, encompassing various manifestations of breast cancer. The validation set, comprising 15% of the data, serves as an interim evaluator, providing feedback on the model's performance during the training phase. It helps in tuning the model parameters without tapping into the test set, thereby preventing information leak and overfitting. The test set, also 15%, is the ultimate benchmark, offering an unbiased assessment of the model's efficacy. This segregation guarantees that the model undergoes training, validation, and testing on separate data subsets, which is fundamental for evaluating its generalization capability and readiness for real-world application.

Data augmentation is a powerful strategy to enhance the dataset's diversity without physically increasing its size. It introduces a variety of transformations to the training images, creating altered copies that retain the same labels. This process is vital for several reasons:

The model is exposed to different orientations of the tissue structures by rotating images. In practice, the orientation of tissue samples under a microscope is arbitrary, so the model should be invariant to rotation. This helps in simulating a more comprehensive range of tissue orientations, improving the model's capacity to identify patterns regardless of their orientation. Zooming in and out simulates the variation in magnification levels that a pathologist might use when examining different regions of a slide. It allows the model to detect features across various scales, enhancing its robustness to variations in the size of pathological structures. Flipping

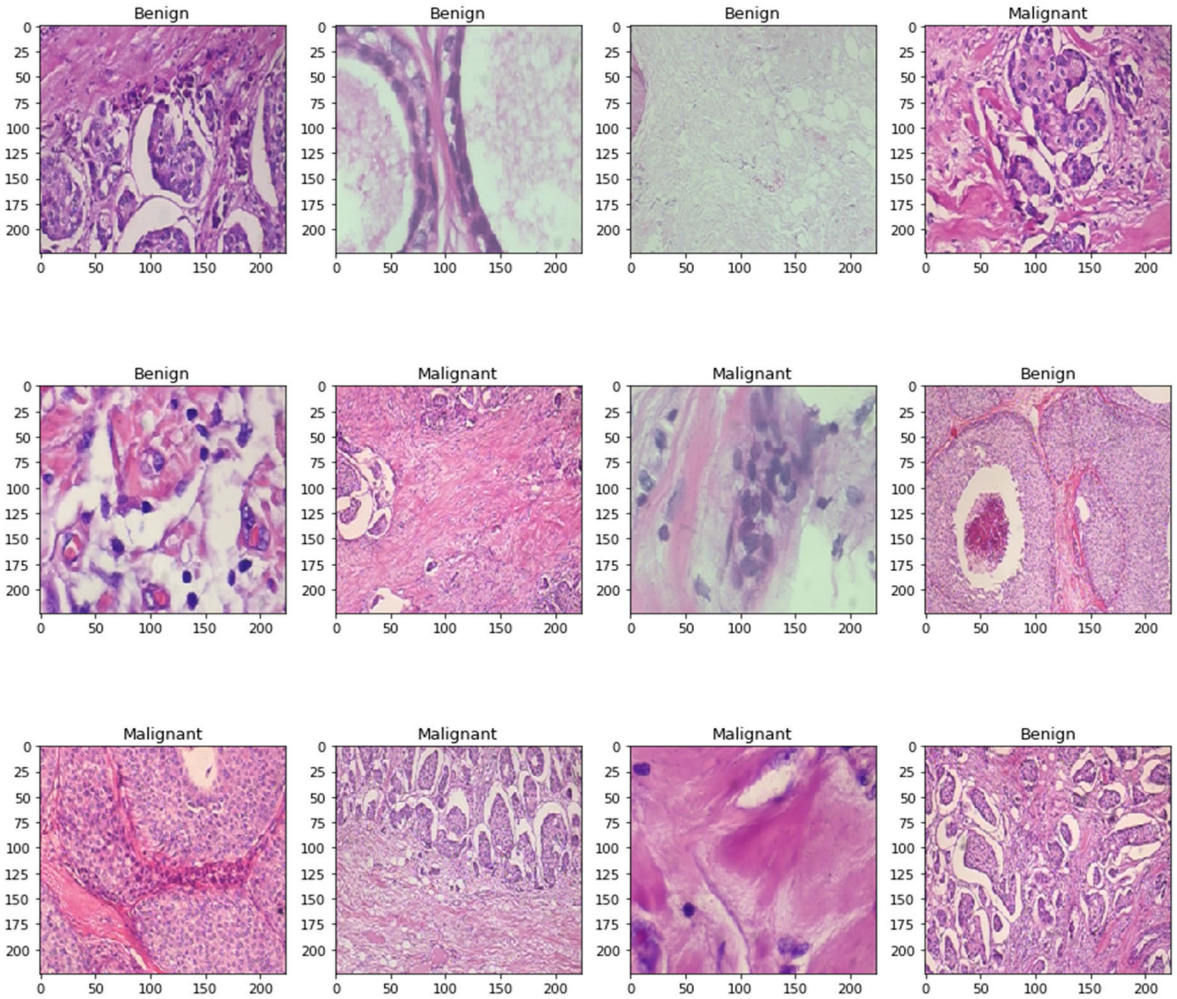

FIGURE 3. Sample histopathological images of different classes in the dataset.

images horizontally and vertically introduces mirror-image variability. In histopathological analysis, the orientation of the sample is not standardized, so the model needs to recognize pathological features regardless of their reflection. This augmentation guarantees that the model's performance remains unbiased by the orientation of the tissue structures. Adjusting brightness and contrast is crucial because staining techniques in histopathology can vary in intensity, and lighting conditions can alter the appearance of samples. By varying these parameters, the model learns to focus on structural features rather than colour intensity, making it adaptable to different staining and imaging conditions. For enhancing model robustness and ensuring generalizability across varied imaging conditions, we implemented a series of data augmentation techniques detailed in Table 3. These procedures are essential for training deep learning models, particularly in medical imaging, where variations in image acquisition frequently occur.

Equations 1,2,3, 4 are commonly used in image processing to perform various transformations and adjustments on digital images.

$$I_{rot} = rotate\,(I, \theta) \tag{1}$$

where,

- I_{rot}*represents* rotated image,
- I is the original image,
- and θ is the rotation angle.

$$I_{zoom} = zoom\,(I, z) \tag{2}$$

where,

- I_{zoom} is the zoomed image,
- I is the original image, and
- z is the zoom factor.

$$I_{flip} = flip\,(I, axis) \tag{3}$$

TABLE 3. Techniques for data augmentation used on the training dataset.

Data Augmentation Method	Description
Normalization	Normalizes the pixel values in the images by subtracting the mean and dividing by the standard deviation.
Random Horizontal Flip	Flips images horizontally with a 50% chance to augment the dataset and introduce variability.
Random Rotation	Rotates the images by up to 0.1 radians (about 5.7 degrees) randomly to simulate different viewing angles.
Random Contrast	Adjusts the contrast of the images by a factor of 0.1 randomly to mimic variations in lighting conditions.
Random Zoom	Zooms into the images randomly up to 20% to mimic closer inspection of regions of interest.

where,

- I_{flip} is the flipped image,
- I is the original image, and
- axis defines the axis along which the image is flipped.

$$I_{bright} = adjust\_brightness\,(I, \beta) \tag{4}$$

where,

- I_{bright} is the brightness-adjusted image,
- I is the original image, and
- β is the brightness adjustment factor.

These augmentation techniques collectively improve the model's robustness and its capacity to generalize from the training data to novel, unseen images, effectively mimicking the variability and unpredictability of real-world clinical data.

B. MODEL ARCHITECTURE

The Patch Extraction Layer serves as the foundational element of the External Attention Transformer (EAT) model. This layer is meticulously designed to mirror the process by which pathologists analyse histopathological slides, where the focus is typically on smaller, specific regions or 'patches' rather than the entire image at once. This methodical approach aids pathologists in identifying disease indicators, an aspect that the EAT model seeks to replicate. By dissecting input images into a grid of distinct patches, the model ensures that each patch, a localized region of the image, contains a subset of the overall visual information. These patches are then flattened, converting the two-dimensional pixel matrices into one-dimensional vectors. This transformation is pivotal as it enables the linear processing of spatial features, facilitating the extraction and analysis of meaningful patterns within each patch [24], [25].

Figure 4 showcases the architecture of the External Attention Transformer (EAT) model, illustrating its key components and data flow. A learnable linear layer is employed to project these flattened patch vectors into a higher-dimensional space, thereby enhancing the model's capability to discern complex features within the patches. Equation 5 defines the dimensions of extracted patches, equation 6 calculates the total patches extracted from the image, equation 7 represents the patch dimensions and equation 8 projects on each extracted patch.

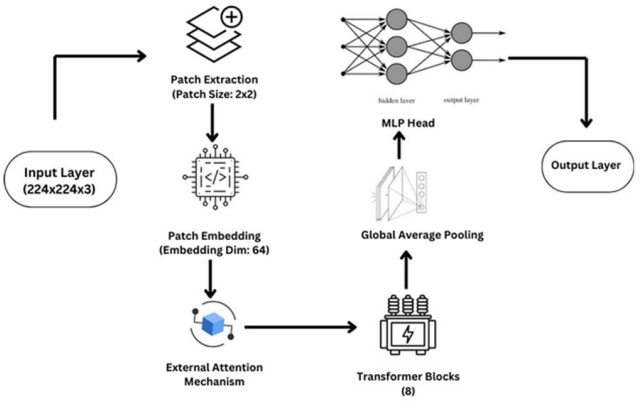

FIGURE 4. The architecture of the External Attention Transformer (EAT) model.

$$Patch\ Size = Patch\ Width \times Patch\ Height \tag{5}$$

where,

- Patch Width and Patch Height define the dimensions of each patch that is extracted from the input image.

$$Number\ of\ Patches = \left(\frac{Image\ Width}{Patch\ Size}\right)^2 \tag{6}$$

where,

- Image Width is the width of the input image, and
- Patch Size is the size of each extracted patch.

The equation calculates the total number of patches extracted from the image.

$$Patch_i = Extract\,(Image, i, Patch\ Size) \tag{7}$$

where,

- 'Image' is the input image from which patches are extracted,
- 'i' is the index of the patch,
- and 'Patch Size' defines the size of each patch.

$$Embedded\ Patch_i = Dense\,(Patch_i, Embedding\ Dim) \tag{8}$$

where,

- $Patch_i$ represents the i-th extracted patch, and
- Embedding Dim is the dimensionality to which the patch is projected.

Central to the innovation of the EAT model is the External Attention Mechanism, a distinctive feature that sets it apart from traditional transformer models. This mechanism is inspired by the cognitive process observed in pathologists,

who shift their focus across different regions of a biopsy slide, concentrating on areas with diagnostic significance. The mechanism consists of two key components: the M-key (Memory Key) and the M-value. The M-key functions as a memory matrix, identifying and storing essential features from the input patches. It is instrumental in learning to assign attention scores to various features, effectively determining the critical elements to focus on within the patches. The M-value complements this by aggregating the attended features, combining them in a manner that is weighted by their respective attention scores. This ensures that the most salient features, as identified by the M-key, significantly influence the model's output, enabling a detailed and nuanced analysis that transcends the capabilities of treating the image as a whole. Equation 9 normalizes the input, equation 10 calculates the attention score between features, equation 11 computes the normalized attention score.

$$LayerNorm\,(x) = \gamma\left(\frac{x-\mu}{\sigma}\right) + \beta \tag{9}$$

where,

- 'x' is the input to be normalized,
- 'γ' and 'β' are learnable parameters, and
- 'μ' and 'σ' represent the mean and standard deviation of the input.

$$e_{ij} = \text{score}\left(H_i, H_j\right) \tag{10}$$

where,

e_{ij} is the attention score between features H_i and H_j.

$$\alpha_{ij} = \frac{\exp\left(e_{ij}\right)}{\sum_{k=1}^{N}\exp\left(e_{ik}\right)} \tag{11}$$

where,

α_{ij} is the normalized attention score,
e_{ij} is the raw attention score, and
N is the number of features.

Following the processing through multiple external attention layers, the model consolidates the attended and extracted features. This aggregation typically involves an average pooling process, which condenses the feature representations from all patches into a singular, cohesive vector. This vector then serves as the input for the Multi-Layer Perceptron (MLP) head, a critical component comprising a series of fully connected layers and non-linear activations. The MLP head refines the processed features, sharpening the distinctions between benign and malignant classifications. It culminates in an output layer equipped with a SoftMax function, which translates the final feature representation into probabilistic predictions corresponding to the two cancer classes: benign and malignant. The role of the MLP head is integral to the model's functionality, as it synthesizes the dispersed yet significant cues into a definitive classification, akin to a pathologist's final diagnostic decision after a thorough examination of various slide regions [26]. This sophisticated integration of features embodies the essence of the model's analytical prowess, underscoring its potential as a transformative tool in the histopathological image analysis. Equation 12 applies a sequence of dense layers and non-linear activations (GELU), equation 13 computes the average of all elements in the input feature map, equation 14 represents the updated memory key matrix obtained by applying the SoftMax function.

$$MLP\,(x) = Dense\,(GELU\,(Dense\,(x))) \tag{12}$$

where,

'x' is the input to the multi-layer perceptron (MLP) which applies a sequence of dense layers and non-linear activations.

$$GlobalAvgPool\,(x) = \frac{1}{N}\sum_{i=1}^{N} x_i \tag{13}$$

where,

'x' is the input feature map, and
'N' is the number of elements in 'x' over which the average pooling is performed.

$$M_k = softmax\,(W_k \cdot X) \tag{14}$$

where,

M_k is the updated memory key matrix,
W_k is the weight matrix associated with the key, and
X represents the input features to the attention mechanism.

C. TRAINING PROCEDURE

The EAT model employs a structured approach to classify histopathological images into benign or malignant categories. Algorithm 1 provides a concise and comprehensive view of the processes included in building and deploying the EAT model for the classifying histopathological images [27].

1) OPTIMIZATION AND LOSS FUNCTION

The training process employs the AdamW optimizer, an enhancement of the traditional Adam optimizer. AdamW introduces weight decay regularization directly into the optimization process, separating the weight decay from the optimization steps. This distinction allows for more precise control over the model's regularization, combating overfitting while maintaining the adaptive learning rate benefits of Adam [28]. It's particularly effective for models with sparse data and helps in fine-tuning pre-trained networks. Equation 15 represents the update rule used in the AdamW optimization algorithm for updating the parameters during training of a neural network.

$$w_{t+1} = w_t - \eta \cdot m_t / \left(\sqrt{v_t} + \epsilon\right) - \lambda \cdot w_t \tag{15}$$

where,

- w_t is the parameter value at time step t,

- η is the learning rate,
- m_t and v_t are the first and second moment estimates in AdamW, respectively,
- ϵ is a small number to prevent division by zero, and λ is the weight decay factor.

The chosen loss function is categorical cross-entropy with label smoothing. This function is well-suited for classification tasks as it quantifies the disparity between the forecasted probability distribution and the actual distribution. Label smoothing incorporates a degree of uncertainty by softening hard targets, which helps prevent the model from becoming excessively confident in its predictions. This uncertainty aids the model in generalizing better to new data, reducing the risk of overfitting to the training set. Equation 16 depicts the cross-entropy loss function, frequently employed in classification tasks to gauge the discrepancy between the true labels and the predicted labels probabilities for each class c.

$$L = -\sum_{c=1}^{M} y_{o,c} \log \left(p_{o,c}\right) \tag{16}$$

where,

- '$y_{o,c}$' is the true label,
- '$p_{o,c}$' is the predicted probability, and
- 'M' is the number of classes.

2) LEARNING RATE SCHEDULING

Learning rate scheduling is a technique that automatically modifies the learning rate throughout the training process. The model employs a dynamic learning rate schedule, where the learning rate is modulated according to the validation loss performance. If the validation loss plateaus or stops improving significantly, the learning rate is lowered. This strategy allows the model to make larger updates when the loss is decreasing and fine-tune with smaller updates as it converges, improving its ability to find an optimal solution and avoiding entrapment in local minima. Equation 17 describes the adjustment of the learning rate.

$$\eta_{new} = \eta \cdot decay\_rate \tag{17}$$

where,

- η_{new} is the adjusted learning rate,
- η is the initial learning rate, and
- decay_rate is the factor by which the learning rate is adjusted.

3) EARLY STOPPING

Early stopping is a regularization method that terminates the training process when the model's performance on the validation set fails to improve after a specified number of consecutive epochs. This method is instrumental in preventing overfitting, as it stops the model from learning noise in the training data beyond a certain point. By tracking the validation loss and ending the training once the loss ceases to decrease, early stopping ensures that the model preserved is the one that performs best on unseen data, not just on the training set. Equation 18 presents a simple stopping criterion

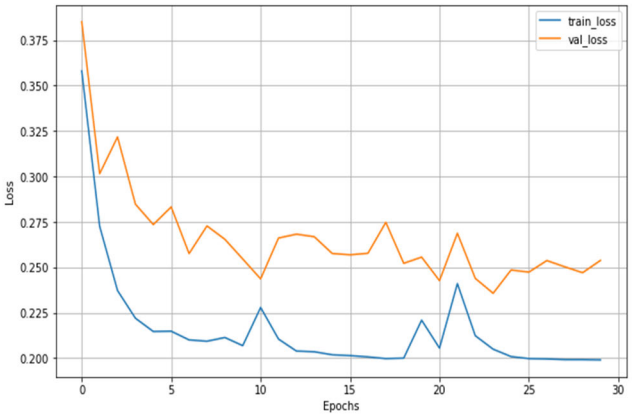

FIGURE 5. Training and validation losses over epochs.

based on validation loss during training. Figure 5 showcases the graphical representation of the training and validation loss over epochs.

$$if\ val\_loss_t > val\_loss_{t-1} : stop \tag{18}$$

where,

- val_loss_t is the validation loss at time step t, and
- val_loss_{t-1} is the validation loss at the previous time step.

The training procedure is meticulously designed to optimize the EAT model's learning process, employing strategies that ensure robustness, generalization, and efficient convergence. These techniques collectively strive to enhance the model's performance, making it a dependable tool for categorizing histopathological images within the scope of diagnosing breast cancer.

D. EVALUATION METRICS

When evaluating the External Attention Transformer Model for categorizing histopathological images of breast cancer, several metrics have been used to comprehensively assess its performance. These metrics encompass Accuracy, Precision, Recall, F1-Score, and the Receiver Operating Characteristic (ROC) Curve, including the Area Under the Curve (AUC).

Accuracy is a crucial metric for assessing classification models, denoting the proportion of accurately predicted observations relative to the total number of observations. It is the most straightforward performance measure and provides an immediate understanding of how well the model is performing overall. It provides a straightforward assessment of the overall performance of the model and offers a quick snapshot of how well the model performs across all classes, which is particularly useful for preliminary assessments. Specifically, accuracy is calculated as shown in equation 19.

$$Accuracy = \frac{Number\ of\ Correct\ Predictions}{Total\ Number\ of\ Predictions} \tag{19}$$

Although accuracy is important, it may not always provide a comprehensive view of the model's performance, particularly

when handling imbalanced datasets. Therefore, it's imperative to assess the model's performance using additional metrics that can provide deeper insights into its predictive capabilities.

In the context of medical diagnostics, precision and recall are particularly significant:

Precision, also referred to as

Positive Predictive Value measures the accuracy of the model's positive predictions. It is crucial to confirm that when the model identifies a case as malignant, it is indeed accurate. High precision is important in reducing false positives, which is critical in clinical settings to prevent undue anxiety or unnecessary treatments for patients. This metric is significant as it aims to minimize the false positive rate, ensuring that patients are spared from unnecessary medical procedures. Equation 20 defines the precision metric, frequently utilized in binary classification tasks to evaluate the model's performance.

$$Precision = \frac{True\ Positives}{True\ Positives + False\ Positives} \tag{20}$$

Recall, also called Sensitivity or True Positive Rate, assesses the model's capability to identify all relevant cases. In medical contexts, high recall is critical to make sure that all potential malignant cases are detected, thereby reducing the risk of overlooking a serious condition. Equation 21 defines the recall metric, commonly used in binary classification tasks to assess the model's performance.

$$Recall = \frac{True\ Positives}{True\ Positives + False\ Negatives} \tag{21}$$

The F1-Score represents the harmonic mean of precision and recall, offering a single metric that balances both aspects [29]. This score is particularly advantageous in situations where the expenses associated with false positives and false negatives are substantial or in cases where there is an imbalance in class distribution. It holds particular value in medical diagnosis scenarios characterized by uneven class distributions. Equation 22 outlines the formula used to compute the F1-score.

$$F1 - Score = 2 \times \frac{Precision \times Recall}{Precision + Recall} \tag{22}$$

The confusion matrix is a commonly used table to illustrate the performance of a classification model [30]. It provides detailed insights into the model's accurate and inaccurate classifications across various classes, showing true positives, false positives, false negatives, and true negatives. This matrix is crucial for assessing the model's performance, especially in detecting any biases or patterns in its predictions.

The Receiver Operating Characteristic (ROC) curve demonstrates how well a binary classifier system can distinguish between classes as its discrimination threshold varies. It is constructed by plotting the true positive rate (recall) against the false positive rate (1 - specificity) [31]. ROC Curve is crucial to understand the trade-offs between sensitivity and specificity, enabling adjustments to the model's threshold that might be necessary to optimize clinical outcomes. Equation 23 defines the True Positive Rate (TPR), and Equation 24 defines the False Positive Rate (FPR), commonly used in binary classification tasks to evaluate the performance of a model.

$$TPR = \frac{TP}{TP + FN} \tag{23}$$

$$FPR = \frac{FP}{FP + TN} \tag{24}$$

where:

- TP: True Positives
- FP: False Positives
- FN: False Negatives
- TN: True Negatives

The Area Under the ROC Curve (AUC) is a comprehensive measure of the model's performance across various classification thresholds. An AUC score of 1 indicates perfect prediction, while 0.5 suggests no discriminative power. Equation 25 defines the Area Under the ROC Curve (AUC) which quantifies the performance of a binary classification model across all possible threshold values.

$$AUC = \int_0^1 TPR\,(t)dt \tag{25}$$

The area under the ROC curve is calculated by integrating the true positive rate (TPR) over all thresholds 't'.

Mean Squared Error (MSE) and Root Mean Squared Error (RMSE) quantify the average squared difference between estimated values and actual values. In classification tasks, they offer insights into the variance of the model's errors. Equation 26 computes the average squared difference between actual values y_i and predicted values $\hat{y}_i$:

$$MSE = \frac{1}{n}\sum_{i=1}^{n}\left(Y_i - \hat{Y}_i\right)^2 \tag{26}$$

Equation 27 calculates the square root of the MSE to yield the RMSE:

$$RMSE = \sqrt{\frac{1}{n}\sum_{i=1}^{n}\left(Y_i - \hat{Y}_i\right)^2} \tag{27}$$

These metrics are useful for assessing the model's accuracy in predicting continuous values, such as in regression tasks.

Mean Absolute Error (MAE) calculates the average size of errors in a set of predictions, without considering their direction [32]. Unlike MSE or RMSE, it is less sensitive to outliers and offers a direct indication of the average error magnitude. Equation 28 computes the average absolute difference between the actual values and the predicted values.

$$MAE = \frac{1}{n}\sum_{i=1}^{n}\left|Y_i - \hat{Y}_i\right| \tag{28}$$

Utilizing these metrics offers a thorough understanding of the model's effectiveness, strong points, and aspects requiring enhancement. This multifaceted evaluation is crucial in developing a model that is both precise and reliable and robust for clinical use. This detailed metric analysis aids in tailoring the

model more effectively to clinical needs, where both accuracy and the ability to differentiate between types of errors are paramount.

IV. EXPERIMENT AND ANALYSIS

The experimentation with the External Attention Transformer Model (EANet) on a dataset of histopathological images has yielded exceptionally promising results, showcasing the model's potential to significantly enhance diagnostic processes in the medical field, especially in differentiating between non-cancerous and cancerous breast cells.

The model demonstrated exceptional accuracy, achieving 99.0% on the test set, highlighting its effectiveness in accurately classifying images. This high degree of precision is essential in medical diagnostics, where the precision of every result could directly impact patient treatment decisions and outcomes. The model is meticulously designed for training procedure using a set of well-defined hyperparameters, essential for ensuring the reproducibility and robustness of our model's performance. The specific training parameters employed are detailed in Table 4, which includes settings such as the learning rate, batch size, and the architecture of our transformer model.

The classification report offers an in-depth evaluation of the model's performance across various classes, highlighting its precision, recall, and F1-scores, which underscore its reliability and robustness. Specifically, the precision of 0.98 for the benign class and a perfect 1.00 for the malignant class indicate demonstrating that the model is dependable in its predictions, with minimal false positives. This is especially critical in a clinical setting, as false positives in the malignant class can cause undue stress and unnecessary treatment for patients. Conversely, recall rates of 1.00 for the benign class and 0.98 for the malignant class indicate the model's strong capability to accurately identify true positive cases. This capability is crucial to ensure no malignant case goes undetected [32]. Figure 6 shows the classification report of the model and Figure 7 shows the graphical representation of different metrics in the model, providing a clear visual comparison of precision, recall, and F1-scores for both benign and malignant classes.

The confusion matrix provides a visual representation of the model's predictions, displaying the counts of true positives, false positives, false negatives, and true negatives. By analyzing the confusion matrix, it becomes evident whether the model tends to misclassify certain classes more frequently or if there are specific areas where its performance can be improved. Figure 8 Confusion Matrix shows that the model correctly identified a high number of benign and malignant cases (high TP), with minimal false positives, indicating it rarely misclassifies benign cases as malignant. Few false negatives demonstrate the model's capability to identify most malignant cases accurately. The high number of true negatives affirms the model's accuracy in classifying non-cancerous images.

TABLE 4. Hyperparameters for training the external attention transformer model.

Parameter	Value	Description
Input Shape	(224, 224, 3)	The dimensions of the input images.
Number of Classes	2	Number of categories for classification.
Weight Decay	0.0001	Regularization parameter to prevent overfitting.
Learning Rate	0.001	Initial learning rate for the optimizer.
Label Smoothing	0.1	Softens the labels as a regularization technique.
Validation Split	20%	Proportion of data used for model validation.
Batch Size	4	The quantity of samples analyzed before the model undergoes an update.
Number of Epochs	30	Total number of complete iterations through the training dataset.
Patch Size	2 x 2	Dimensions of the patches extracted from the input images.
Number of Patches	15,744	Total number of patches extracted from each image.
Embedding Dimension	64	Dimensionality of the embedding space.
MLP Dimension	64	Dimensionality of the Multi-Layer Perceptron layers.
Dimension Coefficient	4	Coefficient for scaling dimensions within the transformer.
Number of Heads	4	Number of attention heads in the transformer model.
Attention Dropout	20%	Dropout rate for attention layers to prevent overfitting.
Projection Dropout	20%	Dropout rate for the projection layers in the model.
Number of Transformer Blocks	8	Total number of transformer layers stacked in the model.

The high true positive rate in both categories suggests effective case identification, crucial for reliable diagnostics. The low false positive rate reduces unnecessary treatments and stress for patients, while the low false negative rate ensures critical conditions are not overlooked. The balanced performance between true positives and true negatives across both categories shows the model maintains consistency without favoring one class over the other. This high true positive rate and low false positive rate are crucial for minimizing unnecessary treatments and ensuring that malignant cases are accurately identified.

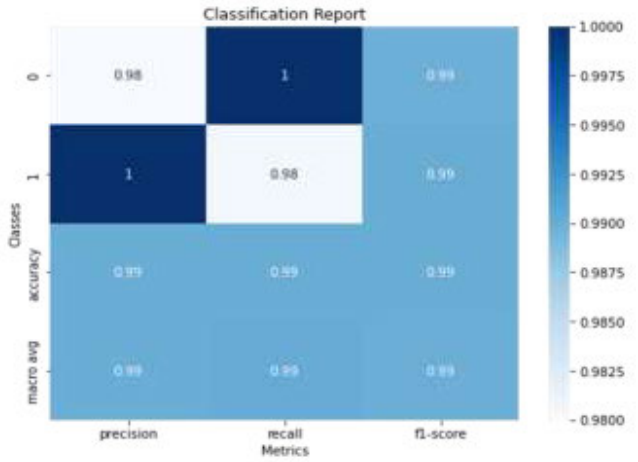

FIGURE 6. Classification report of the EAT Model.

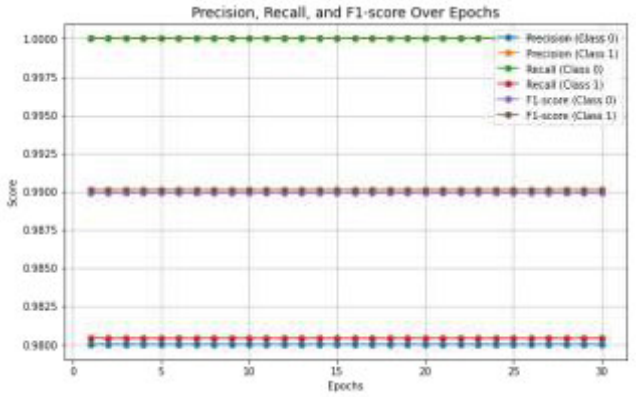

FIGURE 7. Graphical representation of different metrics in the EAT Model.

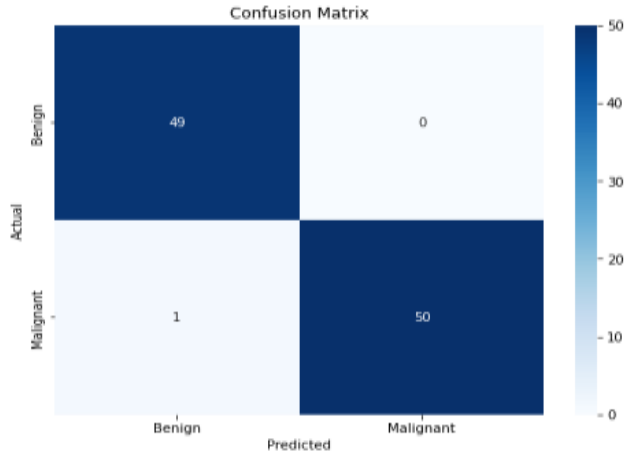

FIGURE 8. Confusion matrix of the EAT model.

Error metrics such as Mean Squared Error (MSE), Root Mean Squared Error (RMSE), and Mean Absolute Error (MAE) all indicate low values, confirming the model's precision and consistency in its predictions across different samples [33]. Such low error rates are indicative of the

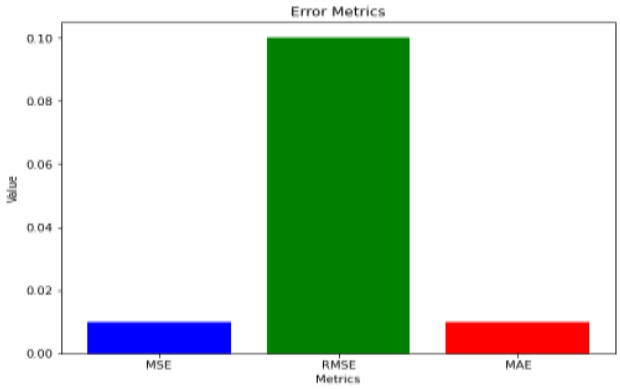

FIGURE 9. Error metrics of the EAT model.

model's potential for reliable application in clinical settings, where the margin for error is minimal. Figure 9 represents the different error metrics.

The model's consistent performance across different metrics underscores its potential as a valuable diagnostic tool for assisting pathologists in rapidly and accurately identifying cancerous cells. This capability could facilitate prompt patient treatment, especially in high-volume medical environments. As an initial diagnostic aid, the tool can help medical professionals effectively prioritize more complex or ambiguous cases.

The Receiver Operating Characteristic (ROC) curve, an essential metric for evaluating performance, was plotted to assess the model's diagnostic capability. The Area Under the Curve (AUC) for the EAT model was 0.98, indicating excellent discrimination between benign and malignant classes. The ROC curve and its AUC offer a comprehensive assessment of the model's performance across various threshold levels, highlighting its sensitivity and specificity in classifying histopathological images. Figure 10 illustrates the ROC curve.

The EANet model demonstrates exceptional performance and potential for practical application in medical diagnostics. Its ability to accurately classify histopathological images with high precision and low error rates suggests that it could be a significant aid in the early detection and treatment of breast cancer, thus contributing to enhanced patient care and outcomes. Future studies could focus on comparing this model's performance with other state-of-the-art models or exploring its applicability to other types of histopathological data, further validating its versatility and effectiveness in medical imaging analysis.

To further understand the model's performance, an analysis of misclassified and correctly classified instances was conducted. This analysis revealed that most misclassifications occurred in images where the histopathological features were subtle or atypical, which presents an inherent challenge in medical image classification.

Figure 11 presents examples of misclassified images, while Figure 12 displays examples of correctly classified images. These figures offer insight into the scenarios where the model

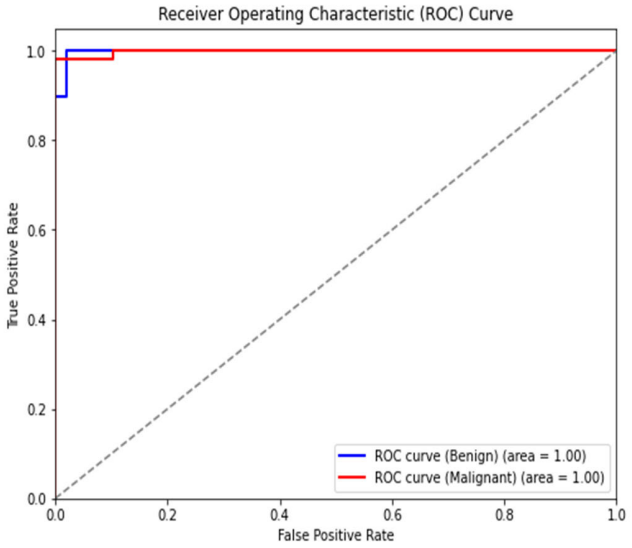

FIGURE 10. ROC curve for the EAT model.

performs well and where it encounters challenges. This visual representation helps in identifying patterns or specific features that may lead to misclassification, offering a pathway for further refinement of the model.

The EAT model's performance was rigorously assessed against existing methodologies, particularly CNN-based models commonly utilized for breast cancer classification tasks. Notably, the EAT model surpassed the standard CNN approach, which achieved a reported accuracy of 95% on the identical dataset. This improvement in accuracy was attributed to the EAT model's capacity to discern salient features within histopathological images through its external attention mechanism. Moreover, the EAT model exhibited superior computational efficiency by processing images in patches and focusing computations only where essential, contrasting with CNNs that compute dense representations for entire images. In addition to accuracy and efficiency, the EAT model demonstrated robustness to variability, showcasing its ability to handle images with diverse staining and quality levels effectively. This resilience stemmed from its attention mechanism, which selectively emphasized regions containing the most relevant information for classification. Furthermore, the model displayed promising generalization capabilities across different datasets, suggesting its potential utility in various clinical settings. Table 5 depicts the comparative analysis of the proposed model compared to the existing models.

To further enhance the clarity and impact of this comparative analysis, Figure 12, illustrating the accuracy scores of the discussed models in a graphical format. This visual aid allows for an immediate and intuitive comparison of the model performances, highlighting the superior accuracy of the EAT model.

In the discussion of the study, the External Attention Transformer Model (EANet) exhibited superior accuracy in classifying histopathological images into benign and malignant categories, achieving an accuracy of 99%. This performance

TABLE 5. Study comparing different approaches.

Author	Techniques	Accuracy
Shemonti Barua et al. (2024) [3]	External Attention Multilayer Perceptron-Based Transformer	95.73%
Anmol Verma et al. (2021) [34]	Automatic deep learning framework	80.4%
D. Banumathy et al. (2021) [35]	Convolutional Neural Networks, particularly ResNet50	94.17%
Agaba Ameh Joseph et al. (2022) [36]	Feature extraction techniques and Deep Neural Network (DNN) classifiers	96% - 97.8%
Mohammad Yosofvand et al. (2023) [37]	U-Net and Mask R-CNN	95%
Umer, Muhammad Junaid et al. (2023) [38]	Deep learning-based solution	92.7%
Nalini Sampath et al. (2023) [39]	Hybrid CNN	96.9%
Harsh Vardhan Guleria et al. (2023) [40]	Variational Autoencoder (VAE), Denoising Variational Autoencoder (DVAE) and Convolutional Neural Network (CNN).	73%
Sameh Zarif et al. (2024) [41]	MobileNet+DenseNet121, MobileNetV2+EfficientNetV2B0, and other deep learning models	96.3%
Soumya Sara Koshy et al. (2024) [42]	Hybrid convolutional neural network model with asymmetric convolutions and Levenberg–Marquardt optimization named as LMHistNet	88%
Wei Wang et al. (2022) [43]	Semi-supervised vision transformer	98.12%
Bhavannrayanna Kolla et al. (2024) [44]	Swin-Transformer V2 architecture	99%
Asmi Sriwastawa et al.(2023) [45]	MaxViT	91.57%
Shehroz Tariq et al. (2024) [46]	Convolutional layers into the ViT model	89.43%
Proposed Model	External Attention Transformer Model (EANet)	99%

surpasses that of traditional deep learning models such as ResNet50 and advanced combinations like MobileNet with DenseNet, which previously demonstrated accuracies ranging from 80.4% to 96.3%. The key advantage of EANet is its external attention mechanism, which efficiently focuses on relevant image features, enhancing accuracy without the complexity and computational overhead associated with other sophisticated models. The high precision and recall scores imply that the model is not only effective in correctly identifying true positive cases but also proficient in minimizing false positives and false negatives. This is particularly important in a clinical setting as high precision ensures that patients are not subjected to unnecessary treatments, while high recall guarantees that almost all malignant cases are detected, thus reducing the risk of missed diagnoses.

Despite these promising results, there are potential limitations in the study. One significant limitation is the dataset's scope. Although the BreaKHis dataset is comprehensive, it might not capture the full diversity of histopathological images encountered in different clinical settings worldwide.

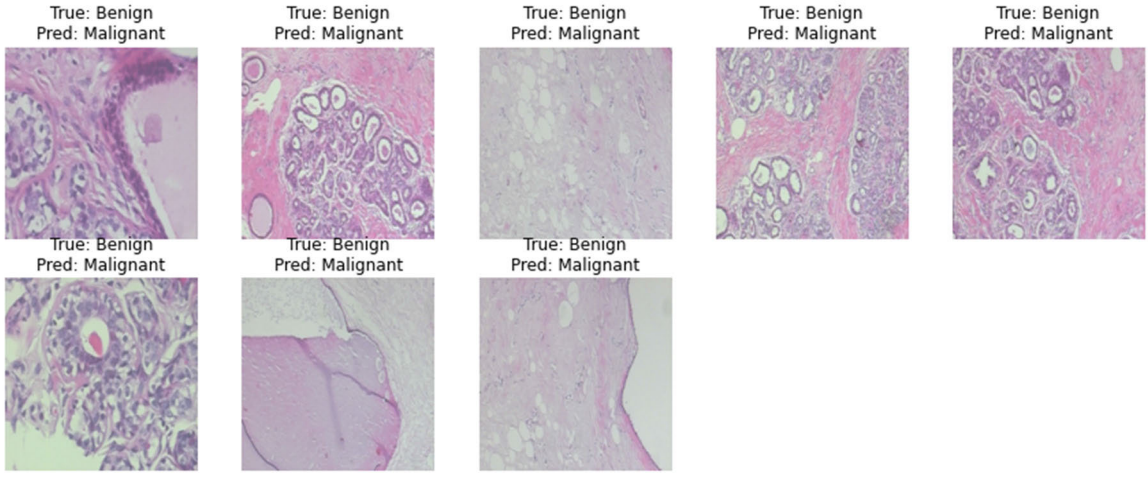

FIGURE 11. Misclassified instances.

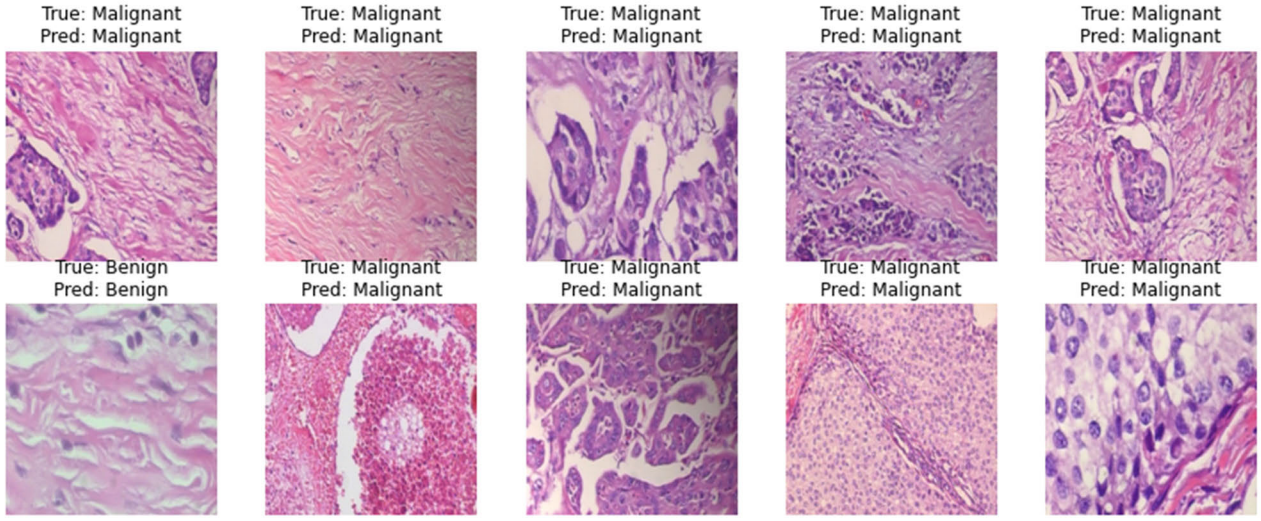

FIGURE 12. Classified instances.

This could impact the model's generalizability to other datasets. Additionally, the study focuses on binary classification (benign vs. malignant), whereas in a real-world scenario, a multi-class classification that includes various subtypes of breast cancer could provide more detailed diagnostic information. Another limitation is the model's interpretability. While the EANet model shows high accuracy, understanding the specific features that drive its decisions could be challenging for clinical practitioners.

To address these limitations, future work could involve expanding the dataset to encompass a wider variety of histopathological images from different sources and developing multi-class classification models that offer more granular diagnostic insights. Enhancing the model's interpretability by integrating explainable AI techniques could also be crucial in gaining the trust of medical professionals. Moreover, conducting validation studies in real-world clinical environments to evaluate the model's practical utility and its impact on diagnostic workflows would be highly valuable. This could involve collaboration with healthcare institutions to integrate the model into routine diagnostic procedures and gather feedback from pathologists.

Ensuring the interpretability of machine learning algorithms is crucial in the medical domain, as it directly impacts clinical decision-making. The External Attention Transformer (EAT) model incorporates features that enhance the transparency of its decision-making processes, particularly using attention mechanisms. These mechanisms are pivotal not only for improving performance but also for enhancing interpretability. The attention mechanism in the EAT model generates a heatmap-like output, highlighting which parts of the histopathological image had the greatest impact on the model's decisions. This allows pathologists and medical experts to visually verify the focus areas of the model,

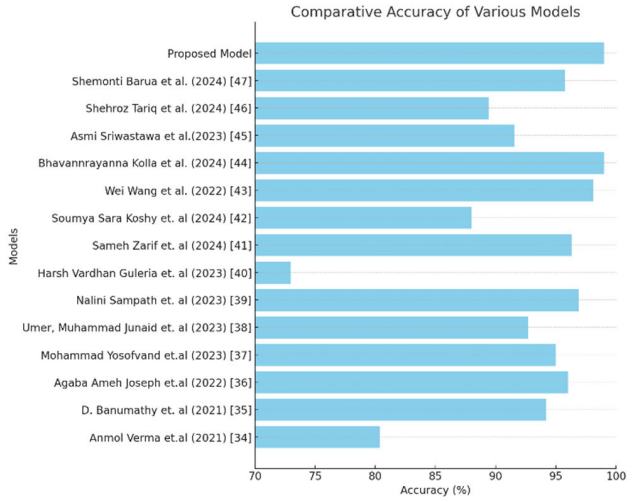

FIGURE 13. Graphical representation of the comparative accuracies.

ensuring alignment with clinically relevant features in the tissue samples. Overlaying these heatmaps on the original images provides a clear and intuitive visualization of the model's focus points. Additionally, domain experts can further validate the model's decisions by reviewing cases where the model's output is juxtaposed with the heatmap outputs, allowing for a detailed examination of the overlap between the model-highlighted areas and known diagnostic markers identified through traditional histopathological analysis. This comparative analysis helps experts evaluate the model's accuracy in real-world diagnostic scenarios.

V. CONCLUSION

In this study, the External Attention Transformer Model (EANet) was employed to classify histopathological images as either benign or malignant. The model attained an outstanding accuracy of 99.0%, accompanied by high precision, recall, and F1-scores for both categories. Specifically, the model's precision for the benign class was 0.98 and 1.00 for the malignant class, while recall rates were 1.00 for benign and 0.98 for malignant. These metrics demonstrate the model's effectiveness and reliability in classifying medical images, which is crucial for diagnosing and planning treatment for breast cancer patients. The low error rates (MSE, RMSE, and MAE) further emphasize the model's consistency and potential for use in clinical settings.

The high precision and recall scores indicate that the model effectively minimizes both false positives and false negatives, ensuring accurate and comprehensive detection of breast cancer. This capability is essential in clinical settings to prevent unnecessary treatments and ensure no malignant cases are overlooked.

Despite these promising results, potential limitations include the scope of the dataset, which may not capture the full diversity of clinical images, and the focus on binary classification rather than multi-class classification. The model's interpretability also poses a challenge for clinical practitioners.

Future research should focus on expanding the dataset to encompass a wider variety of histopathological images sourced from diverse origins, aiming to enhance the model's applicability across different scenarios. Additionally, developing multi-class classification models to offer more detailed diagnostic insights and incorporating explainable AI techniques to enhance the model's interpretability would be advantageous directions for further exploration. Additionally, integrating the model into real-world clinical workflows to assess its practicality and impact on diagnostic processes would be invaluable. Enhancing and understanding the interpretability of the model and how it makes decisions process could also be pivotal in gaining trust from medical professionals and ensuring its broader acceptance in healthcare settings.

The success of the EANet model in yhis study emphasizes the potential of advanced machine learning techniques. to make substantial contributions to medical diagnostics, particularly in histopathological image analysis. The model's high accuracy and reliability demonstrates its capability to serve as a robust tool for Early detection and accurate diagnosis of breast cancer, potentially resulting in timelier and more effective treatment strategies. This research not only underscores progress in the intersection of AI and healthcare but also sets the stage for future innovations that could revolutionize patient care and outcomes in oncology and beyond. The ongoing integration of AI into healthcare promises transformative advancements, and this study marks a significant stride forward on that promising path.

ACKNOWLEDGMENT

This research work was supported by the Vellore Institute of Technology (VIT), Vellore, Tamil Nadu, India. The authors express their sincere gratitude to VIT for providing the necessary resources and facilities to carry out this study.

REFERENCES

[1] M. B. Daly, E. Rosenthal, S. Cummings, R. Bernhisel, J. Kidd, E. Hughes, A. Gutin, S. Meek, T. P. Slavin, and A. W. Kurian, "The association between age at breast cancer diagnosis and prevalence of pathogenic variants," *Breast Cancer Res. Treatment*, vol. 199, no. 3, pp. 617–626, Apr. 2023, doi: 10.1007/s10549-023-06946-8.

[2] U. Naseem, J. Rashid, L. Ali, J. Kim, Q. E. U. Haq, M. J. Awan, and M. Imran, "An automatic detection of breast cancer diagnosis and prognosis based on machine learning using ensemble of classifiers," *IEEE Access*, vol. 10, pp. 78242–78252, 2022, doi: 10.1109/ACCESS.2022.3174599.

[3] S. Barua and M. S. Islam, "Breast cancer image classification using external attention multilayer perceptron-based transformer," in *Proc. 3rd Int. Conf. Advancement Electr. Electron. Eng. (ICAEEE)*, Apr. 2024, pp. 1–6, doi: 10.1109/icaeee62219.2024.10561857.

[4] A. U. Haq, J. P. Li, A. Saboor, J. Khan, S. Wali, S. Ahmad, A. Ali, G. A. Khan, and W. Zhou, "Detection of breast cancer through clinical data using supervised and unsupervised feature selection techniques," *IEEE Access*, vol. 9, pp. 22090–22105, 2021, doi: 10.1109/ACCESS.2021.3055806.

[5] M. Ebrahim, A. A. H. Sedky, and S. Mesbah, "Accuracy assessment of machine learning algorithms used to predict breast cancer," *Data*, vol. 8, no. 2, p. 35, Feb. 2023, doi: 10.3390/data8020035.

[6] J. V. Tembhurne, A. Hazarika, and T. Diwan, "BrC-MCDLM: Breast cancer detection using multi-channel deep learning model," *Multimedia Tools Appl.*, vol. 80, nos. 21–23, pp. 31647–31670, Jul. 2021, doi: 10.1007/s11042-021-11199-y.

[7] S. Bhise, S. Gadekar, A. S. Gaur, S. Bepari, D. Kale, and S. Aswale, "Detection of breast cancer using machine learning and deep learning methods," in *Proc. 3rd Int. Conf. Intell. Eng. Manage. (ICIEM)*, Apr. 2022, pp. 1–6, doi: 10.1109/ICIEM54221.2022.9853080.

[8] S. Iqbal and A. N. Qureshi, "Deep-hist: Breast cancer diagnosis through histopathological images using convolution neural network," *J. Intell. Fuzzy Syst.*, vol. 43, no. 1, pp. 1347–1364, Jun. 2022, doi: 10.3233/jifs-213158.

[9] S. Mohapatra, S. Muduly, S. Mohanty, J. V. R. Ravindra, and S. N. Mohanty, "Evaluation of deep learning models for detecting breast cancer using histopathological mammograms images," *Sustain. Oper. Comput.*, vol. 3, pp. 296–302, Jan. 2022, doi: 10.1016/j.susoc.2022.06.001.

[10] S. Safdar, M. Rizwan, T. R. Gadekallu, A. R. Javed, M. K. I. Rahmani, K. Jawad, and S. Bhatia, "Bio-imaging-based machine learning algorithm for breast cancer detection," *Diagnostics*, vol. 12, no. 5, p. 1134, May 2022, doi: 10.3390/diagnostics12051134.

[11] S. Nagdeote and S. Prabhu, "A model to perform prediction based on feature extraction of histopathological images of the breast," *Multimedia Tools Appl.*, vol. 83, no. 6, pp. 18119–18146, Jul. 2023, doi: 10.1007/s11042-023-16245-5.

[12] A. Maleki, M. Raahemi, and H. Nasiri, "Breast cancer diagnosis from histopathology images using deep neural network and XGBoost," *Biomed. Signal Process. Control*, vol. 86, Sep. 2023, Art. no. 105152, doi: 10.1016/j.bspc.2023.105152.

[13] Y. Shi, L. T. Olsson, K. A. Hoadley, B. C. Calhoun, J. S. Marron, J. Geradts, M. Niethammer, and M. A. Troester, "Predicting early breast cancer recurrence from histopathological images in the Carolina breast cancer study," *NPJ Breast Cancer*, vol. 9, no. 1, p. 15-00597, Nov. 2023, doi: 10.1038/s41523-023-00597-0.

[14] H. Kode and B. D. Barkana, "Deep learning- and expert knowledge-based feature extraction and performance evaluation in breast histopathology images," *Cancers*, vol. 15, no. 12, p. 3075, Jun. 2023, doi: 10.3390/cancers15123075.

[15] Y. Gu, M. Wang, Y. Gong, X. Li, Z. Wang, Y. Wang, S. Jiang, D. Zhang, and C. Li, "Unveiling breast cancer risk profiles: A survival clustering analysis empowered by an online web application," *Future Oncol.*, vol. 19, no. 40, pp. 2651–2667, Dec. 2023.

[16] Y. Wei, D. Zhang, M. Gao, Y. Tian, Y. He, B. Huang, and C. Zheng, "Breast cancer prediction based on machine learning," *J. Softw. Eng. Appl.*, vol. 16, no. 8, pp. 348–360, 2023.

[17] G. Sajiv, G. Ramkumar, S. Shanthi, A. Chinnathambi, and S. A. Alharbi, "Predicting breast cancer risk from histopathology images using hybrid deep learning classifier," *Med. Eng. Phys.*, early access, Mar. 2024, Art. no. 104149, doi: 10.1016/j.medengphy.2024.104149.

[18] A. B. Nassif, M. A. Talib, Q. Nasir, Y. Afadar, and O. Elgendy, "Breast cancer detection using artificial intelligence techniques: A systematic literature review," *Artif. Intell. Med.*, vol. 127, May 2022, Art. no. 102276, doi: 10.1016/j.artmed.2022.102276.

[19] C. H. Barrios, "Global challenges in breast cancer detection and treatment," *Breast*, vol. 62, pp. S3–S6, Mar. 2022, doi: 10.1016/j.breast.2022.02.003.

[20] N. M. U. Din, R. A. Dar, M. Rasool, and A. Assad, "Breast cancer detection using deep learning: Datasets, methods, and challenges ahead," *Comput. Biol. Med.*, vol. 149, Oct. 2022, Art. no. 106073, doi: 10.1016/j.compbiomed.2022.106073.

[21] J. Bai, R. Posner, T. Wang, C. Yang, and S. Nabavi, "Applying deep learning in digital breast tomosynthesis for automatic breast cancer detection: A review," *Med. Image Anal.*, vol. 71, Jul. 2021, Art. no. 102049, doi: 10.1016/j.media.2021.102049.

[22] S. A. Alanazi, M. M. Kamruzzaman, M. N. I. Sarker, M. Alruwaili, Y. Alhwaiti, N. Alshammari, and M. H. Siddiqi, "Boosting breast cancer detection using convolutional neural network," *J. Healthcare Eng.*, vol. 2021, pp. 1–11, Apr. 2021, doi: 10.1155/2021/5528622.

[23] S. Sharmin, T. Ahammad, M. A. Talukder, and P. Ghose, "A hybrid dependable deep feature extraction and ensemble-based machine learning approach for breast cancer detection," *IEEE Access*, vol. 11, pp. 87694–87708, 2023, doi: 10.1109/ACCESS.2023.3304628.

[24] R. L. R. Coripuna, D. I. H. Farías, B. O. M. Ortiz, L. C. Padierna, and T. C. Fraga, "Machine learning for the analysis of conductivity from mono frequency electrical impedance mammography as a breast cancer risk factor," *IEEE Access*, vol. 9, pp. 152397–152407, 2021, doi: 10.1109/ACCESS.2021.3122948.

[25] A. Saber, M. Sakr, O. M. Abo-Seida, A. Keshk, and H. Chen, "A novel deep-learning model for automatic detection and classification of breast cancer using the transfer-learning technique," *IEEE Access*, vol. 9, pp. 71194–71209, 2021, doi: 10.1109/ACCESS.2021.3079204.

[26] J. Ahmad, S. Akram, A. Jaffar, M. Rashid, and S. M. Bhatti, "Breast cancer detection using deep learning: An investigation using the DDSM dataset and a customized AlexNet and support vector machine," *IEEE Access*, vol. 11, pp. 108386–108397, 2023, doi: 10.1109/ACCESS.2023.3311892.

[27] P. E. Jebarani, N. Umadevi, H. Dang, and M. Pomplun, "A novel hybrid K-means and GMM machine learning model for breast cancer detection," *IEEE Access*, vol. 9, pp. 146153–146162, 2021, doi: 10.1109/ACCESS.2021.3123425.

[28] D. N. Elsheakh, O. M. Fahmy, M. Farouk, K. Ezzat, and A. R. Eldamak, "An early breast cancer detection by using wearable flexible sensors and artificial intelligent," *IEEE Access*, vol. 12, pp. 48511–48529, 2024, doi: 10.1109/ACCESS.2024.3380453.

[29] S. Aziz, K. Munir, A. Raza, M. S. Almutairi, and S. Nawaz, "IVNet: Transfer learning based diagnosis of breast cancer grading using histopathological images of infected cells," *IEEE Access*, vol. 11, pp. 127880–127894, 2023, doi: 10.1109/ACCESS.2023.3332541.

[30] T. R. Mahesh, A. Thakur, M. Gupta, D. K. Sinha, K. K. Mishra, V. K. Venkatesan, and S. Guluwadi, "Transformative breast cancer diagnosis using CNNs with optimized ReduceLROnPlateau and early stopping enhancements," *Int. J. Comput. Intell. Syst.*, early access, vol. 17, no. 1, Jan. 2024, doi: 10.1007/s44196-023-00397-1.

[31] F. Azour and A. Boukerche, "Design guidelines for mammogram-based computer-aided systems using deep learning techniques," *IEEE Access*, vol. 10, pp. 21701–21726, 2022, doi: 10.1109/ACCESS.2022.3151830.

[32] N. Routray, S. K. Rout, B. Sahu, S. K. Panda, and D. Godavarthi, "Ensemble learning with symbiotic organism search optimization algorithm for breast cancer classification and risk identification of other organs on histopathological images," *IEEE Access*, vol. 11, pp. 110544–110557, 2023, doi: 10.1109/ACCESS.2023.3322222.

[33] S. Misra, S. Jeon, R. Managuli, S. Lee, G. Kim, C. Yoon, S. Lee, R. G. Barr, and C. Kim, "Bi-modal transfer learning for classifying breast cancers via combined B-mode and ultrasound strain imaging," *IEEE Trans. Ultrason., Ferroelectr., Freq. Control*, vol. 69, no. 1, pp. 222–232, Jan. 2022, doi: 10.1109/TUFFC.2021.3119251.

[34] A. Verma, A. Panda, A. K. Chanchal, S. Lal, and B. S. Raghavendra, "Automatic deep learning framework for breast cancer detection and classification from H&E stained breast histopathology images," in *Data Science*. Singapore: Springer, 2021, pp. 215–227, doi: 10.1007/978-981-16-1681-5_14.

[35] D. Banumathy, O. I. Khalaf, C. A. T. Romero, P. V. Raja, and D. K. Sharma, "Breast calcifications and histopathological analysis on tumour detection by CNN," *Comput. Syst. Sci. Eng.*, vol. 44, no. 1, pp. 595–612, 2023, doi: 10.32604/csse.2023.025611.

[36] A. A. Joseph, M. Abdullahi, S. B. Junaidu, H. H. Ibrahim, and H. Chiroma, "Improved multi-classification of breast cancer histopathological images using handcrafted features and deep neural network (dense layer)," *Intell. Syst. Appl.*, vol. 14, May 2022, Art. no. 200066, doi: 10.1016/j.iswa.2022.200066.

[37] M. Yosofvand, S. Y. Khan, R. Dhakal, A. Nejat, N. Moustaid-Moussa, R. L. Rahman, and H. Moussa, "Automated detection and scoring of tumor-infiltrating lymphocytes in breast cancer histopathology slides," *Cancers*, vol. 15, no. 14, p. 3635, Jul. 2023, doi: 10.3390/cancers15143635.

[38] M. J. Umer, M. Sharif, M. Alhaisoni, U. Tariq, Y. Jin Kim, and B. Chang, "A framework of deep learning and selection-based breast cancer detection from histopathology images," *Comput. Syst. Sci. Eng.*, vol. 45, no. 2, pp. 1001–1016, 2023, doi: 10.32604/csse.2023.030463.

[39] N. Sampath and N. K. Srinath, "Breast cancer detection from histopathological image dataset using hybrid convolution neural network," *Int. J. Model., Simul., Sci. Comput.*, early access, Mar. 2023, doi: 10.1142/s1793962324410034.

[40] H. V. Guleria, A. M. Luqmani, H. D. Kothari, P. Phukan, S. Patil, P. Pareek, K. Kotecha, A. Abraham, and L. A. Gabralla, "Enhancing the breast histopathology image analysis for cancer detection using variational autoencoder," *Int. J. Environ. Res. Public Health*, vol. 20, no. 5, p. 4244, Feb. 2023, doi: 10.3390/ijerph20054244.

[41] S. Zarif, H. Abdulkader, I. Elaraby, A. Alharbi, W. S. Elkilani, and P. Pławiak, "Using hybrid pre-trained models for breast cancer detection," *PLoS ONE*, vol. 19, no. 1, Jan. 2024, Art. no. e0296912, doi: 10.1371/journal.pone.0296912.

[42] S. S. Koshy and L. J. Anbarasi, "LMHistNet: Levenberg–Marquardt based deep neural network for classification of breast cancer histopathological images," *IEEE Access*, vol. 12, pp. 52051–52066, 2024, doi: 10.1109/ACCESS.2024.3385011.
[43] W. Wang, R. Jiang, N. Cui, Q. Li, F. Yuan, and Z. Xiao, "Semi-supervised vision transformer with adaptive token sampling for breast cancer classification," *Frontiers Pharmacol.*, early access, vol. 13, Jul. 2022, doi: 10.3389/fphar.2022.929755.
[44] B. Kolla and P. Venugopal, "An integrated approach for magnification independent breast cancer classification," *Biomed. Signal Process. Control*, vol. 88, Feb. 2024, Art. no. 105594, doi: 10.1016/j.bspc.2023.105594.
[45] A. Sriwastawa and J. A. A. Jothi, "Vision transformer and its variants for image classification in digital breast cancer histopathology: A comparative study," *Multimedia Tools Appl.*, vol. 83, no. 13, pp. 39731–39753, Oct. 2023, doi: 10.1007/s11042-023-16954-x.
[46] S. Tariq, R. Raza, A. B. Sargano, and Z. Habib, "Magnification independent breast cancer analysis using vision transformer," *Multimedia Tools Appl.*, early access, Jul. 2024, doi: 10.1007/s11042-024-19685-9.

K. VANITHA (Member, IEEE) received the B.E. and M.E. degrees (CSE) and the Ph.D. degree in computer science engineering from Anna University, Chennai, India, in 2008, 2011, and 2019, respectively. She is currently an Associate Professor with the Department of Computer Science Engineering, Faculty of Engineering, Karpagam Academy of Higher Education, Coimbatore. She has 13 years of teaching experience. Since 2011, she has published more than 32 international journals and conference papers in her specializations. Her research interests include MANET, network security, data science, and machine learning. She is an active member of various professional bodies, such as IEEE and IAENG. She received one Best Paper Award at the IEEE Conference. She is an active reviewer of reputed journals and conferences.

A. MANIMARAN received the Bachelor of Science degree from Bharathidasan University, Tamil Nadu, in 2006, the Master of Computer Applications degree from Anna University, in 2009, and the Ph.D. degree from Bharathidasan University, in 2018. He is currently an Assistant Professor and a dedicated Researcher with the Department of Mathematics, VIT-AP University, Andhra Pradesh. He is committed to mentoring the next generation of scholars. He has ten years of teaching experience and four years of research experience. He has published 25 research papers in reputed national and international journals and conferences. His research interests include machine learning, deep learning, NLP, and data science. In addition to his professional endeavors, he serves as a reviewer for prestigious journals in the fields of data science and artificial intelligence. He is also an Active Member of the Association for Computing Machinery (ACM) and the Computer Society of India (CSI), where he engages in networking opportunities and stays abreast of the latest developments in the field.

K. CHOKKANATHAN received the M.C.A., M.E., M.Phil., and Ph.D. degrees. He is currently an Associate Professor and the Head of the AI Department, Madanapalle Institute of Technology and Science, Madanapalle, Andhra Pradesh. He is having 24 years of academic experience and 12 years of research experience. He has published around 25 international journals, including Scopus, Web-of-Science, and SCI. He has presented around 13 research papers in international conferences. Also, he has published five patents, two text books, and two book chapters. His research interests include network traffic classification, machine learning, and blockchain technology. He chaired as a resource person for many FDPs, webinars, seminars, and STPs.

K. ANITHA is currently an Assistant Professor with the Department of Information Technology, CSI College of Engineering, Ooty, Nilgiris, Tamil Nadu. She is having 15 years of academic experience. She has published around five international journals, including Scopus, Web-of-Science, and SCI. She has presented around three research papers in international conferences. Also, she has published one patent and one text book. Her research interests include network security and machine learning.

T. R. MAHESH (Senior Member, IEEE) is currently an Associate Professor and the Program Head of the Department of Computer Science and Engineering, Faculty of Engineering and Technology, JAIN (Deemed-to-be University), Bengaluru, India. He has to his credit more than 100 research articles in Scopus/WoS and SCIE indexed journals of high repute. He has been the editor of books on emerging and new age technologies with publishers, such as Springer, IGI Global, and Wiley. His research interests include image processing, machine learning, deep learning, artificial intelligence, the IoT, and data science. He served as a reviewer and a technical committee member for multiple conferences and journals of high reputation.

V. VINOTH KUMAR (Member, IEEE) is currently an Associate Professor with the School of Computer Science Engineering and Information Systems (SCORE), Vellore Institute of Technology (VIT), Vellore, India. He is the author/co-author of papers in international journals and conferences, including SCI indexed papers. He has published more than 60 articles in IEEE Access, Springer, Elsevier, IGI Global, and Emerald. His current research interests include wireless networks, the Internet of Things, machine learning, and big data applications. He is an Associate Editor of *International Journal of e-Collaboration* (IJeC) and *International Journal of Pervasive Computing and Communications* (IJPCC) and an editorial member of various journals.

G. N. VIVEKANANDA (Senior Member, IEEE) is currently an Associate Professor with the School of Computer Science Engineering and Information Systems, Vellore Institute of Technology, Vellore. He is a Certified Ethical Hacker, a Microsoft Certified Educator, a Certified Professional, and an IBM Certified Academic Associate. He has published many articles in peer-reviewed journals. His research interests include AI and ML, networks, security, the IoT, and blockchain technologies. He is a Life Member of various prestigious organizations, such as IEI, CSI, and ISTE. He was a recipient of the IEI Young Engineers Award in 2022. He chaired sessions and was the guest of honor at the conferences. He has acted as a resource person for more than 80 programs.